



# Molecular orientation in individual electrospun nanofibers measured via polarized Raman spectroscopy

Leon M. Bellan\*, Harold G. Craighead

School of Applied and Engineering Physics, Cornell University, 212 Clark Hall, Ithaca, NY 14853, United States

## ARTICLE INFO

### Article history:

Received 29 January 2008

Received in revised form 25 April 2008

Accepted 28 April 2008

Available online 15 May 2008

### Keywords:

Electrospinning  
Polarized Raman  
Orientation

## ABSTRACT

Using polarized Raman spectroscopy, we have recorded Raman spectra from individual electrospun Nylon-6 nanofibers. Analysis of these single-fiber spectra, compared to those of unoriented and oriented Nylon-6 films, indicates significant molecular orientation. Because electrospinning produces fibers in a jet with a large strain rate, this molecular orientation is expected. We present quantitative measurements of molecular orientation in a single nanofiber and compare these to those of film samples. Such measurements could yield information about the uniformity of the electrospinning process and resulting fibers, and may also allow comparison between spectrally measured orientation functions and single-fiber mechanical properties.

© 2008 Elsevier Ltd. All rights reserved.

## 1. Introduction

Electrospinning is a technique for forming microfibers and nanofibers from a wide range of polymeric materials using an electrically forced fluid jet [1,2]. In most systems, the strong elongational flow of the fluid jet results in fibers with high degrees of molecular orientation. The extent of this orientation, as well as its uniformity over the length of the fiber, will have an impact on the material properties of the fiber. Several previous studies have observed molecular orientation in large bundles of fibers using X-ray scattering and diffraction techniques [3–6], polarized Raman spectroscopy [4], and birefringence analysis [7]. Other studies have measured mechanical properties of both electrospun fiber mats [8,9] and individual electrospun fibers [5,8,10]. Transmission electron diffraction techniques have been used to attempt to characterize the microstructure of single fibers [3,6,11], but because of problems due to sample thickness and damage to the fiber caused by the incident beam, the resulting data are either non-existent or have a very poor signal-to-noise ratio; thus quantitative molecular orientation measurements using this method are yet to be published. While measurements of molecular orientation performed on large bundles of fibers provide information about the average molecular orientation over several fibers (or, from a different point of view, over several distantly spaced positions of material deposited from the same jet), these measurements cannot provide much information about the uniformity of this orientation.

Electrospinning jets exhibit complex fluid behavior and various types of instabilities [12–14], resulting in fibers with properties with a wide distribution. For example, a single electrospinning jet depositing fibers from a single solution will form fibers with a wide range of diameters [8,15]. It is likely that other parameters, such as density, crystallinity, and molecular orientation, would exhibit a similarly wide distribution; this has been suggested by transmission electron microscopy (TEM) studies [6]. Moreover, it would be useful to compare mechanical measurements taken from a single, short (tens of microns) section of fiber to a measurement of molecular orientation taken from the same fiber section.

In this article we describe the measurement of molecular orientation from polarized Raman spectra from an individual electrospun Nylon-6 fiber. We acquire spectra using four polarization geometries ( $X|X$ ,  $Y|Y$ ,  $X|Y$ ,  $Y|X$ ) using the notation “incident polarization|analyzed polarization” and the axes shown in Fig. 1. We qualitatively compare these spectra to those from unoriented and oriented Nylon-6 films, as well as to spectra taken from large bundles of Nylon-6 fibers [16]. We also present results from quantitative analysis of the single-fiber spectra, yielding the  $P2$  (sometimes called the Herman’s function) and  $P4$  orientation functions.

## 2. Experimental methods

Raman spectra were acquired using a Renishaw inVia micro-Raman system using incident light at 488 nm from a Melles Griot laser (Melles Griot 543-AP-A01, incident power 4–5 mW) focused on the sample using a 50× 0.75 NA objective (Leica). A  $\lambda/2$  waveplate (Thorlabs) was sometimes inserted in the beam path prior to

\* Corresponding author. Tel.: +1 607 255 6286; fax: +1 607 255 7658.  
E-mail address: [lmb79@cornell.edu](mailto:lmb79@cornell.edu) (L.M. Bellan).

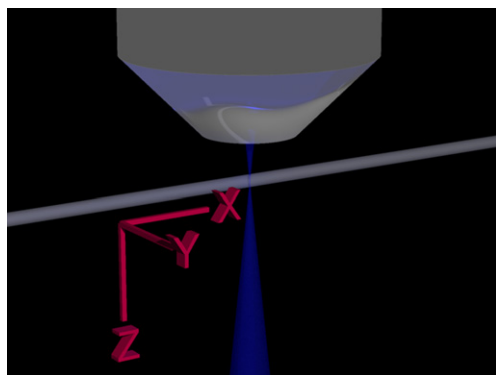


**Fig. 1.** Geometry of polarized Raman experiments. A laser beam passes through a microscope objective and is focused on an isolated fiber. The backscattered light is collected with the same objective, and passes to the Raman spectrometer.

the microscope entrance to allow rotation of the polarization of the incident radiation. A  $\lambda/2$  waveplate and polarizer (part of the micro-Raman system) were at times inserted after the notch filter to select the appropriate polarization of the analyzed light. Using this setup, we were able to take spectra in four geometries (X|X, X|Y, Y|X, and Y|Y) from any sample. For the purpose of this article, we define Z as the axis of incident radiation, X as the axis of orientation in the sample, and Y as the axis transverse to the sample orientation (Fig. 1). A backscattering geometry was used in all cases. The spot diameter of the incident radiation was approximately  $4\ \mu\text{m}$ .

Control experiments were performed using unoriented Nylon-6 film (Kenylon 6250, KNF Corporation). Spectra were taken from the unoriented film and from film that had been stretched on

a homebuilt system. For the experiments with film, the  $\lambda/2$  waveplate for the incident beam was not used and the film was rotated with respect to the incident polarization. Nanofibers were electrospun from a solution of 30% Nylon-6 (Aldrich) in formic acid (Mallinckrodt) using the scanned electrospinning technique [17]. In this technique, a droplet of solution is placed on an electrified (6–10 kV) microfabricated silicon tip held a distance of 2–4 cm from a grounded substrate. The droplet forms a fluid jet which is accelerated towards a grounded substrate. As the solvent in the fluid evaporates from the jet, a solid fiber is formed and deposited on the grounded substrate. We used a chopper motor to rotate the substrate through the jet to isolate and orient the fibers. A transmission electron microscopy (TEM) grid was used as the collecting substrate so that regions of the fibers would be freely suspended, but over relatively small holes to reduce fiber drift. The grid was glued to a metal washer for ease of handling. The washer was placed on a stack of washers sitting on an XY piezo stage system (Physik Instrumente M662.4) mounted on a rotation stage. This rotation stage was centered using the manual microscope stage on the micro-Raman system.

### 3. Results and discussion

Spectra over the  $800\text{--}1800\ \text{cm}^{-1}$  range from control experiments performed on unoriented and oriented Nylon-6 films are shown in Fig. 2. By observing the changes in the spectra from the X|X and Y|Y geometries one can qualitatively determine that stretching the film induces anisotropy, as expected. We were able to identify the peaks expected in Nylon-6: the s(C–CO) peak at  $934\ \text{cm}^{-1}$ , the s(C–C) peaks at 1001, 1040, 1063, 1078, 1127, and

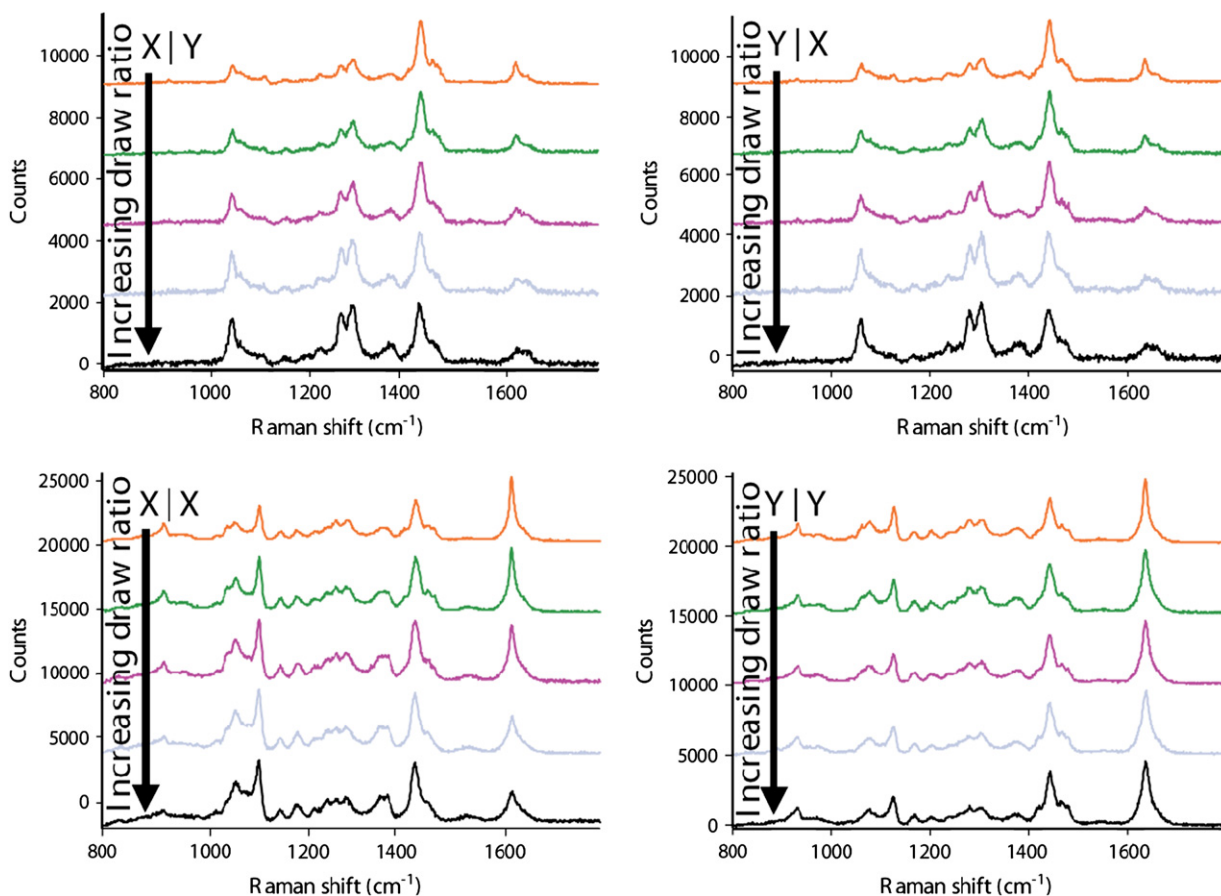


**Fig. 2.** Spectra from unoriented and oriented Nylon-6 films with four polarization geometries. As the draw ratio increases, the material becomes more anisotropic, manifested by differences between the X|X and Y|Y spectra.

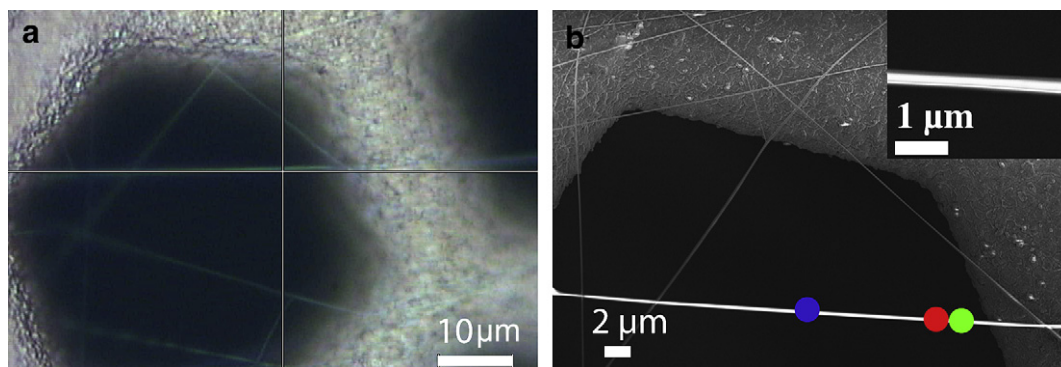


**Fig. 3.** (a) Brightfield image of individual electrospun Nylon-6 fiber (under crosshairs) from micro-Raman system and (b) SEM image of the same fiber. Higher magnification SEM images (inset) indicate a fiber diameter of approximately 280 nm. The colored dots indicate approximate positions corresponding to the spectra in Fig. 4.

1168  $\text{cm}^{-1}$ , the  $w(\text{CH}_2) + t(\text{CH}_2)$  peaks at 1204 and 1230  $\text{cm}^{-1}$ , the Amide III peak at 1278  $\text{cm}^{-1}$ , the  $t(\text{CH}_2)$  peak at 1306  $\text{cm}^{-1}$ , the  $w(\text{CH}_2)$  peak at 1379  $\text{cm}^{-1}$ , the  $b(\text{CH}_2)$  peak at 1443  $\text{cm}^{-1}$ , the Amide II peak at 1555  $\text{cm}^{-1}$ , and the Amide I peak at 1635  $\text{cm}^{-1}$  [16,18] (where  $s$  indicates stretching,  $w$  indicates wagging,  $t$  indicates twisting and  $b$  indicates bending).

We were also able to obtain Raman spectra from individual electrospun Nylon-6 nanofibers. Fig. 3 shows a single fiber as observed using the brightfield illumination on the micro-Raman system (Fig. 3a) and the same fiber imaged using a scanning electron microscope (SEM) (Fig. 3b) after Raman spectra were obtained. From SEM imaging, the diameter of this fiber was determined to be 280 nm. The fiber was oriented horizontally using a rotation stage and then positioned in the beam using linear piezo stages. Due to

the difficulty in perfectly centering the rotation stage, the polarization of the incident light with respect to the sample orientation was rotated using the incident beam  $\lambda/2$  waveplate as opposed to rotating the sample. Raman spectra from the four geometries for this fiber (over the 800–1700  $\text{cm}^{-1}$  range) are shown in Fig. 4. Spectra were taken at three places along the fiber; these are indicated by different colors. Each spectrum corresponds to a single “SynchroScan” extended scan acquisition of 200 s and a binning value of 3. Variations between the spectra at the three positions may be due to actual variations in the fiber, variations in the fiber position in the laser spot (in the X, Y, and Z (focus) directions), and noise in the system. The background in the spectra may be due to noise inherent to the Raman system, fluorescence of the fiber, and background from the air surrounding the fiber (note that the strong

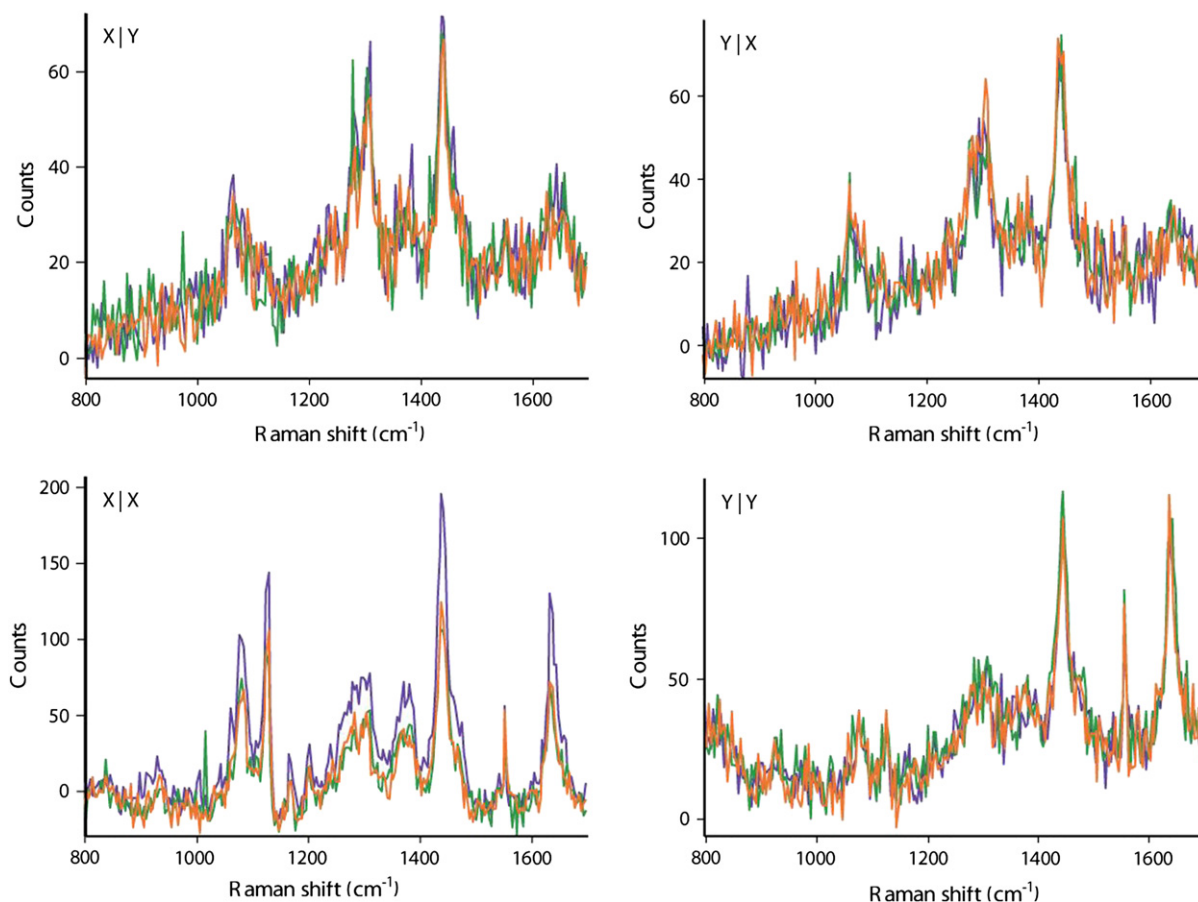


**Fig. 4.** Polarized Raman spectra from the isolated electrospun Nylon-6 nanofiber shown in Fig. 3. The differences between the X|X and Y|Y spectra indicate significant anisotropy.

peak at  $1555\text{ cm}^{-1}$  in the X|X and Y|Y spectra is likely due to oxygen in the air [19], as the Amide II peak at the same wavenumber should be weak for all geometries [16,18] and the  $1555\text{ cm}^{-1}$  peak is seen in spectra taken without any fiber under the microscope objective). By noting the significant qualitative differences between the X|X and Y|Y spectra, we observe that there is significant molecular orientation in the fiber.

Previous studies using Raman spectroscopy to analyze Nylon-6 bundles indicate that electrospinning Nylon-6 results in the  $\gamma$  crystalline form of the material [16]; this is in agreement with studies employing X-ray diffraction to analyze electrospun Nylon-6 nanofibers [20]. This crystalline form, unlike the  $\alpha$  form typically observed in bulk and solution-cast films, is observed in high-speed melt-spun Nylon-6 filament and is the dominant crystalline form for fibers formed under high stress [21]. In electrospun Nylon-6 fibers, the chain axis of the  $\gamma$  crystalline form is parallel to the fiber axis [22]. Upon comparison to spectra in Ref. [12], some regions (the orange spectrum in Fig. 5) showed spectra strongly indicative of a  $\gamma$  form, while others (the blue spectrum in Fig. 5) appeared to possess shapes slightly different from the pure  $\gamma$  form. While all regions demonstrate significant molecular orientation, the crystallinity and orientation of crystals may vary significantly [6], which may account for the variation in spectrum shape.

Polarized Raman spectroscopy may be used as a tool to quantitatively measure molecular orientation by calculating the  $P2$  and  $P4$  orientation functions [23–28]:

$$P2 = \frac{1}{2} \left( 3 \langle \cos^2 \theta \rangle - 1 \right)$$

$$P4 = \frac{1}{8} \left( 35 \langle \cos^4 \theta \rangle - 30 \langle \cos^2 \theta \rangle + 3 \right)$$

We have chosen to analyze the s(C–C) peak at  $\sim 1120$ – $1130\text{ cm}^{-1}$  as it has a low depolarization ratio but a measurable peak height in all spectra, indicates a vibration along the molecular backbone, and is easily isolated from other peaks. Peaks were fit using the WiRE software from Renishaw, and the resulting values (along with the depolarization ratio, 0.075, measured from the unoriented film) were used to solve a series of equations for  $P2$  and  $P4$  according to two slightly different treatments [23,27]. We also calculate a qualitative orientation parameter,  $P_{\text{qual}} = 1 - (I_{yy}/I_{xx})$ , where  $I_{xx}$  and  $I_{yy}$  are the intensities of the peak in the X|X and Y|Y spectra, respectively [26]. The results for the unoriented film, the

**Table 1**

$P2$  and  $P4$  values calculated using two methods and a qualitative orientation parameter from polarized Raman spectra from several samples

Sample	$P2$ (Refs. [22,26])	$P4$ (Refs. [22,26])	$P_{\text{qual}}$
Unoriented film	0.03, 0.03	0.08, 0.06	0.08
Highly oriented film	0.20, 0.14	0.31, 0.33	0.35
Red position	0.88, 0.88	-1.7, -0.91	0.78
Blue position	0.87, 1.1	-0.53, -0.55	0.86
Green position	0.66, 0.83	-0.92, -1.0	0.75
Another fiber (not shown)	$0.59 \pm 0.06$ , $0.65 \pm 0.07$	$-2.2 \pm 0.4$ , $-2.1 \pm 0.3$	$0.65 \pm 0.06$

most highly oriented film, and several positions along an individual electrospun fiber are shown in Table 1. In order to determine the standard deviation of this measurement technique, 10 sets of four spectra were obtained from a single position on another fiber deposited from the same solution at a different time. The resulting orientation function values, along with the standard deviations, are reported in Table 1. For this set of data, the  $\langle \cos^2 \theta \rangle$  and  $\langle \cos^4 \theta \rangle$  values were  $0.67 \pm 0.04$  and  $0.07 \pm 0.09$ , respectively (using the method outlined in Ref. [18]). We observed no correlation between the calculated orientation values and the set number, indicating that the incident radiation was not measurably altering the microstructure over this timescale.

Though the quantitative analysis described above yields reproducible values, the quantitative results for the electrospun nanofiber samples fall outside the allowed range for the  $P4$  function. For a distribution in which all molecules point along the same angle,  $\langle \cos^4 \theta \rangle = \langle \cos^2 \theta \rangle^2$  and thus  $P4 = (1/18)(35P2^2 - 10P2 - 7)$ . In the other extreme, a randomly oriented sample will have both  $P2$  and  $P4$  equaling 0. It can be shown using Schwartz's inequality that  $|\langle \cos^2 \theta \rangle|^2 \leq \langle \cos^4 \theta \rangle \leq \langle \cos^2 \theta \rangle$ , which imposes a range on the value of  $P4$  for a given value of  $P2$  [29]. Though the film samples yield proper  $P2$  and  $P4$  values, the  $P4$  values in Table 1 for the electrospun nanofiber samples all fall outside the allowed range. We believe that this is due to the high background and poor signal-to-noise ratio (SNR) in the electrospun nanofiber spectra, especially in the X|Y and Y|X spectra where the peak is difficult to resolve over the background. This may also explain the anomalous  $P2$  value of 1.1 obtained for the blue position. It is also possible that birefringence effects may be altering the relative intensities in the spectra so as to cause the calculations to yield anomalous results.

The values in Table 1 can be compared to orientation function values measured in other Nylon-6 systems, such as highly drawn fibers produced using conventional spinning techniques. Previous work investigating orientation in both Nylon-6,6 and Nylon-6 fibers that were drawn at room temperature post-spinning indicates that the  $P2$  orientation function rapidly approaches its maximum value of 1 at draw ratios less than 10 [30–32]. Estimates of the draw ratio in electrospinning jets are of the order of  $\sim 10,000$  [12], and the Deborah numbers in these systems are quite high [33], suggesting that the molecular orientation in electrospun fibers should be similar to, if not exceed that of highly drawn melt-spun fibers.

#### 4. Conclusion

We have obtained polarized Raman spectra for a single electrospun Nylon-6 nanofiber which indicate a significant degree of molecular orientation. These spectra qualitatively agree with those taken from drawn Nylon-6 film, and show features similar to those in previous studies on bundles of electrospun Nylon-6 (known to be in the  $\gamma$  crystalline form). We calculated the  $P2$  and  $P4$  orientation functions with the data we have obtained from individual fibers. The quality of the current quantitative results is limited by the spectra quality, and thus we sometimes obtain anomalous values for the orientation functions  $P2$  and  $P4$ . Future work will focus on

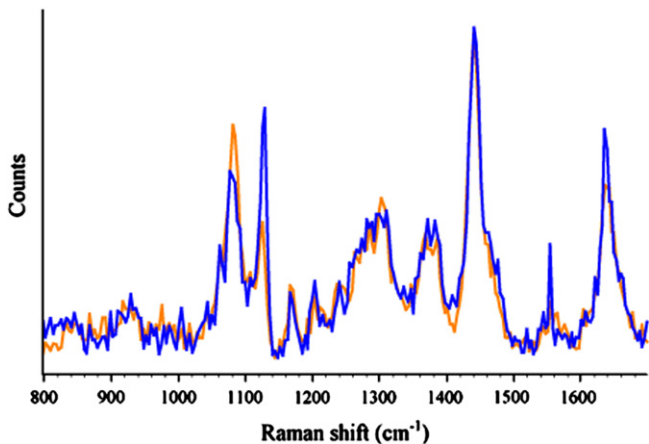


**Fig. 5.** X|X spectra from two different fibers, demonstrating the difference in shape. The spectra were scaled to fit in the same window. The blue spectrum is from the fiber indicated in Fig. 3, and the orange spectrum is from the fiber referred to at the bottom of Table 1.

optimizing the experimental setup and acquiring spectra from a larger set of fibers in order to allow comparison between deposition parameters (take-up velocity, driving voltage, electrospinning solution, etc.). We have observed reproducible differences in the spectra taken from different fibers suggesting that this technique allows molecular orientation measurement from isolated, micron-length areas of individual nanofibers and may give insight into the uniformity of both the electrospinning process and the properties of the resulting nanofibers.

### Acknowledgements

The authors wish to thank Lee Gordon of KNF Corporation for donating unoriented Nylon-6 film, and Richard Borrett, Lynden Archer, and Christopher Umbach for useful discussions regarding Raman spectroscopy. This material is based upon work supported by the Cornell Nanobiotechnology Center (NBTC), a STC Program of the National Science Foundation under Agreement No. ECS-9876771, and the Cornell Center for Materials Research supported by the National Science Foundation under Award Number DMR-0520404. The authors thank the National Science Foundation for partial support of this work under Grant No. HRD-0630456.

### References

- [1] Reneker DH, Chun I. *Nanotechnology* 1996;7(3):216–23.
- [2] Teo WE, Ramakrishna S. *Nanotechnology* 2006;17(14):R89–106.
- [3] Dror Y, Salalha W, Khalfin RL, Cohen Y, Yarin AL, Zussman E. *Langmuir* 2003;19(17):7012–20.
- [4] Kakade MV, Givens S, Gardner K, Lee KH, Chase DB, Rabolt JF. *Journal of the American Chemical Society* 2007;129(10):2777–82.
- [5] Zussman E, Burman M, Yarin AL, Khalfin R, Cohen Y. *Journal of Polymer Science, Part B: Polymer Physics* 2006;44(10):1482–9.
- [6] Dersch R, Liu T, Schaper AK, Greiner A, Wendorff JH. *Journal of Polymer Science, Part A: Polymer Chemistry* 2003;41(4):545–53.
- [7] Catalani LH, Collins G, Jaffe M. *Macromolecules* 2007;40(5):1693–7.
- [8] Li L, Bellan LM, Craighead HG, Frey MW. *Polymer* 2006;47(17):6208.
- [9] Li M, Mondrinos MJ, Gandhi MR, Ko FK, Weiss AS, Lelkes PI. *Biomaterials* 2005;26(30):5999–6008.
- [10] Bellan LM, Kameoka J, Craighead HG. *Nanotechnology* 2005;16(8):1095–9.
- [11] Huang C, Chen S, Lai C, Reneker DH, Qiu H, Ye Y, et al. *Nanotechnology* 2006;17(6):1558–63.
- [12] Reneker DH, Yarin AL, Hao F, Koombhongse S. *Journal of Applied Physics* 2000;87(9, Pt. 1–3):4531–47.
- [13] Shin YM, Hohman MM, Brenner MP, Rutledge GC. *Applied Physics Letters* 2001;78(8):1149–51.
- [14] Shin YM, Hohman MM, Brenner MP, Rutledge GC. *Polymer* 2001;42(25):9955.
- [15] Li D, Xia Y. *Nano Letters* 2003;3(4):555–60.
- [16] Stephens JS, Chase DB, Rabolt JF. *Macromolecules* 2004;37(3):877–81.
- [17] Kameoka J, Orth R, Yang YN, Czaplowski D, Mathers R, Coates GW, et al. *Nanotechnology* 2003;14(10):1124–9.
- [18] Song K, Rabolt JF. *Macromolecules* 2001;34(6):1650–4.
- [19] *Raman spectroscopy of gases and liquids*. Berlin; New York: Springer-Verlag; 1979.
- [20] Fong H, Liu W, Wang C-S, Vaia RA. *Polymer* 2002;43(3):775–80.
- [21] Samon JM, Schultz JM, Wu J, Hsiao B, Yeh F, Kolb R. *Journal of Polymer Science, Part B: Polymer Physics* 1999;37(12):1277–87.
- [22] Liu Y, Cui L, Guan F, Gao Y, Hedin NE, Zhu L, et al. *Macromolecules* 2007;40(17):6283–90.
- [23] Huang K, Archer LA, Fuller GG. *Review of Scientific Instruments* 1996;67(11):3924–30.
- [24] Purvis J, Bower DI. *Journal of Polymer Science: Polymer Physics Edition* 1976;14(8):1461–84.
- [25] Jen S, Clark NA, Pershan PS, Priestley EB. *The Journal of Chemical Physics* 1977;66(10):4635–61.
- [26] Lefevre T, Rousseau ME, Pezolet M. *Canadian Journal of Analytical Sciences and Spectroscopy* 2005;50(1):41–8.
- [27] Rousseau ME, Lefevre T, Beaulieu L, Asakura T, Pezolet M. *Biomacromolecules* 2004;5(6):2247–57.
- [28] George T. *Journal of Raman Spectroscopy* 1984;15(2):103–8.
- [29] Samori B, Thulstrup EW, North Atlantic Treaty Organization. *Scientific Affairs Division. Polarized spectroscopy of ordered systems*. Dordrecht; Boston: Kluwer Academic Publishers; 1988.
- [30] Salem DR, Moore RAF, Weigmann HD. *Journal of Polymer Science, Part B: Polymer Physics* 1987;25(3):567–89.
- [31] Salem DR. *Structure formation in polymeric fibers*. Munich, Cincinnati: Hanser, Hanser Gardner Publications; 2001.
- [32] Vasanthan N, Ruetsch SB, Salem DR. *Journal of Polymer Science, Part B: Polymer Physics* 2002;40(17):1940–8.
- [33] Bellan LM, Craighead HG, Hinestroza JP. *Journal of Applied Physics* 2007;102(9):094308.